Comparison between PHITS and beam physics codes calculations in support of FRIB dipole magnet design

Dali Georgobiani, Marc Hausmann, Mauricio Portillo, Reginald Ronningen
Facility for Rare Isotope Beams (FRIB), Michigan State University, US

Abstract

The Facility for Rare Isotope Beams (FRIB) at Michigan State University will use projectile fragmentation and induced in-flight fission of heavy ion primary beams at energies of 200 MeV/u and higher and at a beam power of 400 kW to generate rare isotope beams for experimental studies in nuclear physics. The production of rare isotope beams during FRIB operations creates a high-radiation environment for the fragment pre-separator superconducting magnets. Therefore, detailed studies of the proposed magnet designs and shielding by both beam physics and radiation transport codes are necessary. We study the radiation power deposition into the 30-degree bending dipole magnet located in the FRIB fragment pre-separator using both the radiation transport code PHITS[1] and the beam physics codes COSY[2] and LISE++[3]. Preliminary results from these approaches are in reasonable agreement. The results of our calculations are important to magnet design.

Introduction

The 400 kW heavy-ion primary beam impinges on the production target located in the target assembly, as shown in Figure 1. A part of the beam reacts with the target and produces rare isotopes as reaction products. The reaction products and the remainder of the primary beam are transported through the post-target shield, three focusing quadrupole magnets, and the sextupole-octupole magnet before reaching the first 30-degree dipole magnet. There they spatially separate into different beam components. Figure 1 shows these major beamline components of the FRIB hot cell pre-separator. The beam dump intercepts the primary beam and the undesired fragments are stopped by associated fragment catchers. If the primary beam and the undesired fragments do not stop in these locations, the potential to cause damage exists. Magnetic field settings for very neutron-rich light rare isotopes lead to large deflections of the primary beam in the dipole, as well as beam focusing conditions that can cause unwanted beam losses. When the primary beam with the residual power of ~300 kW approaches the magnet aperture limit, the accuracy of the simulation becomes important. The primary beam has a certain power density and spatial distribution, while the reaction products have parameters differing from the parameters of the primary beam. The path region for the beam should be wide enough to avoid losses; however, ample shielding is required to minimise radiation heating of the helium cryostat that keeps the superconducting coils cold. The method used here addresses the necessary issues.

Figure 1. An engineering drawing of an elevation view of the FRIB hot cell pre-separator

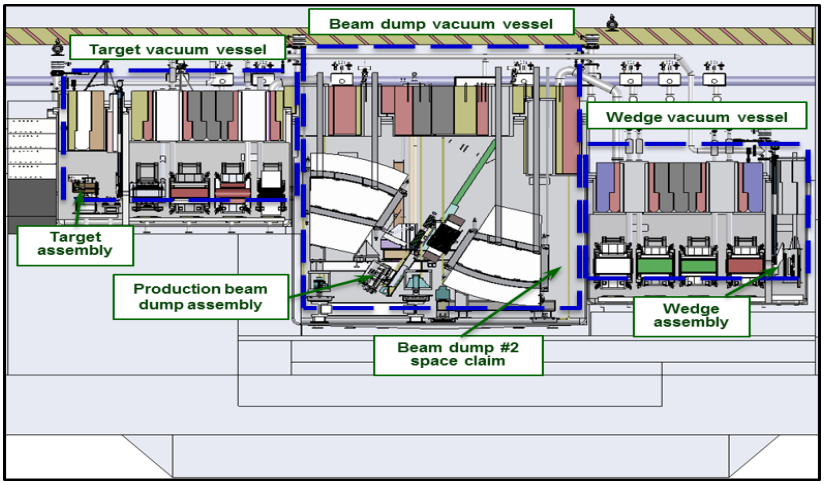

The pre-separator consists of target, beam dump, and wedge vacuum vessels, containing the beam line components: the target assembly, the post-target magnet shield, beam focusing quadrupoles, beam bending dipoles, the beam dump, sextupole-octupoles, and the wedge assembly.

Calculation input and methodology

Beam parameters and code inputs

The radiation transport code PHITS [1] and beam optics codes COSY [2] and LISE^{++} [3] results are compared to validate the codes against each other. The code COSY is used to calculate the maps and optimise the beam transport conditions throughout the system. The maps are calculated to fifth order and the focusing conditions are optimised by varying quadrupoles, sextupoles and octupoles. The maps are then transferred to the code LISE++ which uses the maps for beam transport calculations, and in addition, can do Monte Carlo simulation of the beam particle interactions with matter. This includes the reaction products in the target, but only accounts for charged particles in their ground state; i.e. neutrons, gammas, pions and other secondary particles are not accounted for.

Each of these codes has certain strengths and weaknesses in the context of this work. The COSY maps used by LISE^{++} include the magnet fringe fields, whereas PHITS uses a hard edge approximation and first order simulation of trajectories. LISE^{++} uses beam-matter interaction models that have been frequently tested for the energy regime being considered here. The PHITS code system has the advantage that it tracks events that happen when a particle is lost to the surrounding components in the beam line, such as energy loss and further production which is used to account for activation and damage in the material. On the other hand, LISE^{++} simply ignores effects after a beam particle is lost any aperture in the beamline.

The calculations used for this study focus only on an ^{18}O beam incident on a 2.48 g/cm^2 graphite target at a beam energy of 200 MeV/u and 400 kW of beam power. The magnet fields are optimised to transport a beam of 8 T-m beam rigidity with the product ^{8}He. We use COSY to minimise unwanted losses yet maintain good transmission throughout the separator for ^{8}He. This production setting is expected to give the largest deflection of the primary beam to the bottom side of the dipole. Best match between available models for angular and energy straggling is selected between PHITS and LISE++ in order to make fair side by side comparisons of the straggling effects.

Table 1 presents angular and energy straggling, energy loss, and reaction product models used in LISE^{++} and PHITS calculations. Table 2 shows the comparison of the angular and energy straggling RMS values calculated for the primary beam and a selected

set of fragments. Table 3 compares the average energies of the primary beam calculated after the target. For the purpose of these studies, we find that RMS values calculated after the target for both the primary beam and fragments, as well as average energies, are in reasonable agreement.

Table 1. Angular and energy straggling, energy loss, and reaction product models used in LISE^{++} and PHITS calculations

Model setting	LISE^{++}	PHITS
Angular straggling	ATIMA [4]	ATIMA
Energy straggling	ATIMA	ATIMA
Energy loss	ATIMA	SPAR [6]
Reaction products	Tarasov Model [5]	JAM [7], QMD [8], BERTINI [9]

Table 2. Angular (a-rms) and energy straggling (E-rms) RMS values calculated with LISE^{++} and PHITS for the primary beam and fragments

	LISE^{++}	PHITS	LISE^{++}	PHITS
Beam or Fragment	a-rms [mrad]		E-rms [MeV]	
^{18}O (primary)	3.2	5.1	4.3	4.9
^{16}O	24	15	83	62
^{12}C	35	26	113	100
^{13}N	32	26	105	99

Table 3. Average energy of the primary beam after the target

LISE^{++}	PHITS
E average [MeV]	
2920	2914

Dipole mechanical design and radiation transport models

Mechanical design drawings of the 30-degree bending dipole magnet used to develop the model used in the radiation transport calculations are presented in Figure 2 (panels **a** and **b**). The area of focus in the lower exit corner of the dipole is shown in panel **a** (red circle). Panel **c** depicts a part of the radiation transport model used in the calculations. The radiation transport model supports calculations of losses to all critical components, including the surrounding shielding in the hot cell. Here, the first 30-degree bending dipole, beam dump, sextupole-octupole, and the second 30-degree bending dipole are shown. Most unwanted particles are stopped by the beam dump. A fraction of the beam is lost directly to the bottom blocker and consists mostly of secondary products generated from the primary beam at the target.

Figure 2. Mechanical design drawings of the 30-degree bending dipole (panels a and b) and radiation transport model of the dipole and surrounding beam line components (panel c)

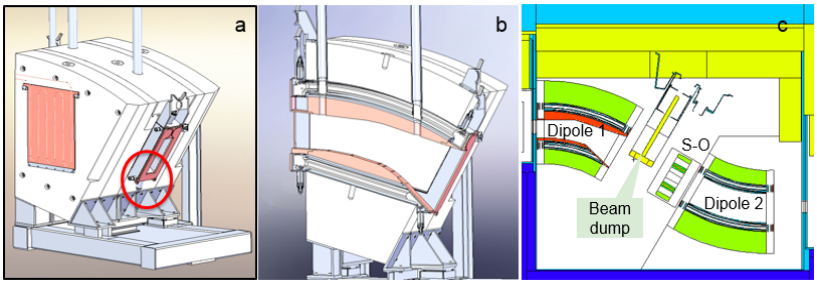

Red circle (panel a) shows the area where the beam hits the dipole in this particular beam setting scenario. Beam blockers optimised to minimise power loss into coils and cryostats are shown in panel b (light pink parts) and in panel c (red parts).

Results of calculations

Beam optics

Beam transport comparisons between LISE^{++} and PHITS results have been performed for reaction products. As an example, beam envelopes for ^{12}C fragments calculated are presented in Figure 3. The similarity in trajectories indicates that the beam optics and the fragment distributions are similar in both calculations.

Figure 3. Beam envelopes for ^{12}C fragments from target for PHITS (top) and LISE^{++} (bottom)

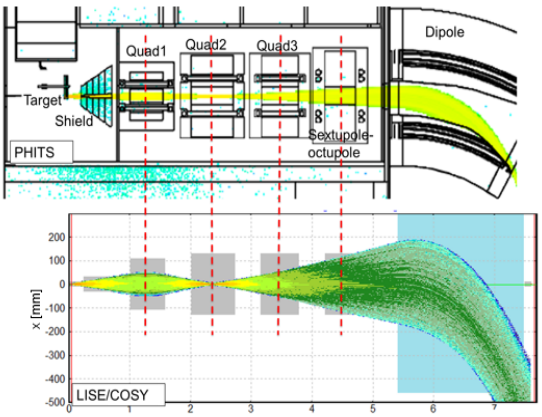

LISE^{++} x-values are in beam co-ordinates; therefore, the dipole bend curvature is not imposed Gray areas in the bottom plot correspond to the apertures of the quadrupoles.

Flux maps and power deposition into the beam blockers

Flux maps from LISE++ and from PHITS calculations are shown in Figure 4. Power deposition to the lower blocker was extracted for each calculation. For losses at the bottom blocker, we obtain 3 kW from LISE^{++} and 2.1 kW from PHITS. The lower value can be explained by the smaller angular spread of reaction products using the ATIMA model within PHITS. The flux distributions are similar and the results of the power deposition calculations are in reasonable agreement.

Figure 4. Flux maps from (left) LISE^{++} and (right) PHITS

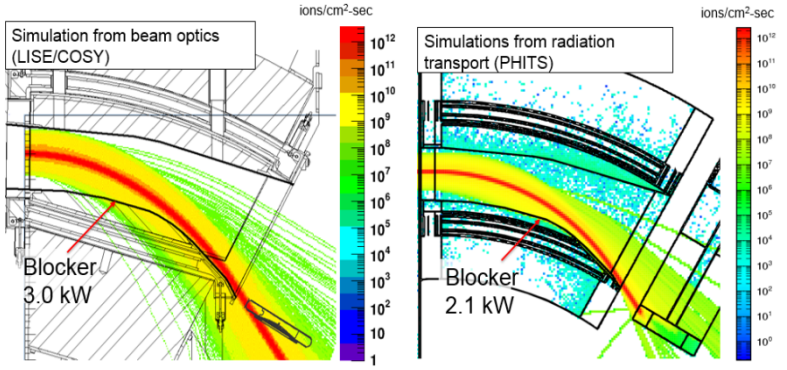

Both the primary beam ^{18}O and reaction products are presented.

Conclusions

The radiation transport code PHITS - with selected settings for straggling and energy loss parameters, as well as its fragment production model was validated against beam optics codes LISE++/COSY to support operational flexibility at FRIB. Beam interference conditions in surrounding components were identified and resolved as follows:

- increasing width of dipole exit window opening so that primary beam clears magnet hardware safely;
- adding top and bottom beam blockers inside of dipole gap to stop intense fragments near the primary beam and reduce the radiation heat load to cryostat;
- optimising the blocker shape to minimise direct beam losses while maintaining adequate shielding;
- developing beam optics settings to minimise losses to all surrounding dipole components;
- calculating induced thermal losses with PHITS to aid in the design of water and helium cooling.

Flux maps from both codes show similar flux distributions. Power deposition to the lower blocker are found to be in reasonable agreement. The radiation transport design is also used in evaluating lifetimes of critical components as well as induced activation.

Summary

Radiation transport (PHITS) and beam optics (LISE^{++}/COSY) codes have been used to calculate beam and fragment distributions, as well as power deposition at the first 30-degree bending dipole magnet located in the FRIB preseparator. Good agreement between the two code systems has been demonstrated. The results from this study provide the design requirements for this magnet in terms of the beam conditions. The current design supports the requirements for future operations for the FRIB project.

Acknowledgements

DG would like to express her gratitude to the SATIF-12 organisers for their hospitality. This material is based on work supported by the US Department of Energy Office of Science under Cooperative Agreement DE-SC0000661, the State of Michigan and Michigan State University. Michigan State University designs and establishes FRIB as a DOE Office of Science National User Facility in support of the mission of the Office of Nuclear Physics.

References

[1] T. Sato, K. Niita, N. Matsuda, S. Hashimoto, Y. Iwamoto, S. Noda, T. Ogawa, H. Iwase, H. Nakashima, T. Fukahori, K. Okumura, T. Kai, S. Chiba, T. Furuta, L. Sihver (2013), "Particle and Heavy Ion Transport Code System PHITS, Version 2.52", *J. Nucl. Sci. Technol.* 50:9, 913.

[2] K. Makino, M. Berz (2005), "COSY INFINITY Version 9", *Nucl. Instr. and Meth. Phys. Res.* A 558, 346-350.

[3] O.B. Tarasov, D. Bazin (2008), "LISE^{++}: Radioactive beam production with in-flight separators ", *Nucl. Instr. and Meth. Phys. Res.* B 266, 4557-4664.

[4] web-docs.gsi.de/~weick/atima/.

[5] O.B. Tarasov (2004), "Analysis of momentum distributions of projectile fragmentation products", *Nucl. Phys.* A 734, 536.

[6] T.W. Armstrong, K.C. Chandler (1973), "A Fortran program for computing stopping powers and ranges for muons, charged pions, protons, and heavy ions", ORNL-4869, Oak Ridge National Laboratory, US.

[7] K.Y. Nara, N. Otuka, A. Ohnishi, K. Niita, S. Chiba (1999), "Relativistic nuclear collisions at 10 A GeV energies from p+Be to Au+Au with the hadronic cascade model", *Phys. Rev.* C 61, 024901.

[8] K. Niita, S. Chiba, T. Maruyama, H. Takada, T. Fukahori, Y. Nakahara, A.Iwamoto (1995), "Analysis of the (N,xN) reactions by quantum molecular dynamics plus statistical decay model", *Phys. Rev.* C 52, 2620.

[9] K. Niita, H. Takada, S. Meigo, Y. Ikeda (2001), "High-energy particle transport code NMTC/JAM", *Nucl. Instr. Methods* B 184, 406.